VECTOR FIELD GUIDANCE LAW FOR CURVED PATH FOLLOWING OF AN UNDERACTUATED AUTONOMOUS SHIP MODEL

(DOI No: 10.3940/rina.ijme.2020.a3.609)

Haitong Xu, and **C Guedes Soares** Centre for Marine Technology and Ocean Engineering (CENTEC), Instituto Superior Técnico, Universidade de Lisboa, Portugal

KEY DATES – Submitted: 18/12/19, Final Acceptance: 02/09/20, Published: 07/10/20

SUMMARY

A vector field guidance law and control system for curved path following of an underactuated surface ship model is presented in this paper. In order to obtain the curved path, continuous derivatives piecewise cubic Hermite interpolation is applied for path generation based on the predefined waypoints. A heading autopilot controller is designed based on 2nd order Nomoto's model and its stability is guaranteed by the Diagram of Vyshnegradsky method. The parameters of Nomoto model are estimated using least square support vector machine based on the manoeuvring tests. The vector field guidance law is applied for both straight and curved path-following control of an underactuated surface ship model. In order to demonstrate the performance, the classical guidance law based on line-of-sight, is adopted for comparison. The results show that the vector field method is capable to solve the guidance problem of underactuated surface ships.

NOMENCLATURE

ρ	Density of water (kg m^{-3})
u	The forward velocity (m s^{-1})
v	The transverse velocity (m s^{-1})
χ	Course angle (rad)
χ^f	Course angle of each segment of the trajectory (rad)
χ^e	Entry angle ($0 < \chi^e < 0.5\pi$) (rad)
χ^c	Desired course angle (rad)
τ	Distance of the transition region (m)
y_e	Cross-track errors (m)
(x_{los}, y_{los})	Virtual target point
(w_{xj}, w_{yj})	Waypoints of the trajectory
(x, y)	Real-time coordinate
d	Distance from the next point (m)
k	Constant, $k \geq 1$
u_c	The current's magnitude (m s^{-1})
α	The current's direction (rad)
ψ^d	The desired heading angle (rad)
ψ	The heading angle (rad)
u_r	The relative forward velocity (m s^{-1})
v_r	Relative transverse velocity (m s^{-1})
m	The mass of the ship (kg)
Δ	Constant (m)
β	Drift angle (rad)
U_r	Relative ground speed (m s^{-1})
$X'_{u_r}, X'_{v_r}, X'_{ee}, \cdots$	Hydrodynamic coefficients of surge motion
$Y'_0, Y'_v, Y'_\delta, \cdots$	Hydrodynamic coefficients of sway motion
$N'_0, N'_r, N'_\delta, \cdots$	Hydrodynamic coefficients of yaw motion
f'_1, f'_2, f'_3	Nondimensionalize hydrodynamic forces and moment
c	Weighted average flow speed (m s^{-1})
A_p	The propeller area (m^2)
A_R	The rudder area (m^2)
ω	The wake fraction
$u_{A\infty}$	The induced axial velocity (m s^{-1})
K_T	The propulsive coefficient
D	The propeller diameter (m)
T_1, T_2, T_3	Nomoto time lag
K	Nomoto gain
K_p, K_d, K_i	PID control gain
$\boldsymbol{w}$	Weight matrix
$\boldsymbol{\varphi}(\cdot)$	Kernel function
C	Regularization factor
$\sum_{i=1}^{N} e_i^2$	Empirical error
b	Bias term
$\mathcal{L}(\boldsymbol{w}, b, e_i, \alpha_i)$	Lagrange function

1. INTRODUCTION

Autonomous surface vehicles (ASVs) have been considered a promising technology for the future maritime industry. They have been used both in navy and commercial applications, for example in marine survey, environment monitoring, and marine search and rescue. Autonomous marine vehicles make it possible to carry out the predefined tasks in dangerous or inaccessible places. For autonomous surface vehicles, guidance and control systems play an important role, because their main job is to control the movement to achieve motion control (Xu and Guedes Soares, 2016a).

Path-following or path-tracking control is a classical problem for underactuated marine surface ships. Some researches on path-following control of marine ships can also be found in (Fossen et al., 2015). The predefined

paths are usually defined by waypoints (Fossen, 2011). For the selection of the way-points, some features need to be taken into consideration, such as weather conditions (Vettor and Guedes Soares, 2016), obstacle avoidance (Sato and Ishii, 1998), environment disturbance (Chen *et al*., 2013), ship emissions (Prpić-Oršić *et al*., 2016) and economic requirements (Xu and Guedes Soares, 2018), among others. Path-following control also attracts much attention in other autonomous systems, such as autonomous ground vehicles (Brown *et al*., 2016; Shin *et al.,* 2015), robots (Michałek, 2014; Wu *et al*., 2001) and autonomous airships (Zheng *et al*., 2013).

The predefined trajectory or the path is usually made up of waypoints that are connected with straight lines (Rong *et al*., 2019). But it is impossible to get a smooth transition between two connected straight lines due to its discontinuity in the first derivative (Lekkas and Fossen, 2014). This kind of physical constraint, i.e. the discontinuity, will normally have bad consequences, such as overshoots and oscillations, especially when the ship begins to follow the next segment of the trajectory. Some researchers have been working on these issues. For example, Fossen (2011), suggested to use a circle to connect two straight lines, which can avoid the overshoots to some extent, but the ship cannot navigate through the predefined points if following the path. It is an unacceptable result if vehicles need to handle obstacles avoidance. So, the technology for connecting the waypoints with continuous derivative should be studied for path following control of ships. For example, Lekkas and Dahl (2013) used an extension of Fermat's spiral to produce a second-order continuous derivative trajectory, which also was proved to be suitable for path following. Pythagorean hodographs technology, which was used to generate a flexible path, was discussed by Bruyninckx and Reynaerts, (1997) and by Farouki and Sakkalis, (1990). Dubis's path (Dubins, 1957) is also a good option to solve the discontinuity of the trajectory, but the drawback is that sometimes Dubin's path will be not available for the application (Techy and Woolsey, 2009).

In this paper, piecewise cubic Hermite interpolation is used for path generation. The resulting path can pass through all the predefined waypoints with continuous derivatives and the geometry shape is stable. When the last way-point changes position, it will have a little effect on the previous segments of the path.

Path-following control system is intended to guide the ship to track the path. The accuracy and robustness are the most critical features of a path-following control system, especially considering the existence of external disturbances, such as wind waves and currents (Sujit *et al*., 2014). In the last decade, the Line of Sight (LOS) guidance law and its properties have been studied thoroughly and used for solving the guidance problem of ASVs. Lekkas and Fossen (2013) presented a review of guidance laws for marine vehicles and discussed LOS in detail. Moreira *et al.*, (2007) proposed a dynamic LOS, which aims to improve the convergence speed and stability when ship deviated from the desired path and further studies were presented in Moreira and Guedes Soares, (2014). An extended LOS, which is a bit gentler than the traditional form, was proposed by Loe (2008).

The Vector Field (VF) guidance law is also a robust algorithm, which is widely used for Unmanned Air Vehicles (UAVs). Nelson *et al*. (2006, 2007) studied the path-following problem for an unmanned air vehicle using vector field both in simulation and scaled model tests. The stability of VF was proved using Lyapunov theory by Gonçalves *et al*., (2010). Xu and Guedes Soares (2016a, 2019a) applied the VF guidance law for the straight path following control of ASVs, the results show that VF is a stable and robust method. Xu *et al*. (2019b) presented the concept of path-following of an autonomous ferry using vector field guidance law and AIS history data. It has the ability to guide autonomous ferry to track a straight path (Hinostroza *et al*., 2019).

The design of the autopilot for an autonomous surface vehicle is an important and challenging topic, owing to the unpredictable environmental disturbances. An adaptive fuzzy logic controller was used for the ship autopilot by Velagic *et al.,* (2003). An optimized sliding mode controller using a genetic algorithm was studied by McGookin *et al*., (2000) for course changing and track keeping of an oil tanker. A different approach to use the sliding mode controller was adopted by Perera, and Guedes Soares (2012). Two autopilots based on feedback control and cascade control for a ship tracking a given trajectory is presented by Morawski and Pomirski (1998).

The contribution of this paper is to investigate the vector field guidance law for the curved path following of underactuated ships. The curved path with continuous derivative is generated using piecewise cubic Hermite polynomials. Another contribution is that a model-based heading controller is proposed, and the corresponded parameters are turned using the Vyshnegradsky diagram method. It can be used to find the control parameters considering the stability property. The control model is identified using least square support vector machine (LS-SVM) based on the manoeuvring tests. To compare the performance of look-ahead LOS and VF guidance laws, simulations will be carried out for both cases, following straight paths and continuous curved paths. Comparative analyses will be made based on the heading angles, cross-track errors and rudder deflection angles.

This paper is organised as follows: Section 2 briefly describes the curved path generation using 2 the cubic Hermite polynomials. Section 3 introduces the vector field guidance laws. In section 4, a nonlinear manoeuvring model is given. The autopilot controller is introduced in section 5, and the stability was proved using Vyshnegradsky diagram. The parameter estimation using LS-SVM is also presented in this section. Numerical studies were carried out in section 6. The conclusions are presented in Section 7.

2. PIECEWISE CUBIC HERMITE POLYNOMIALS FOR GENERATING CURVED-PATH

The trajectory is defined by the waypoints, which are usually connected to each other using a straight line in the Cartesian coordinate system. The straight path is simple and can be implemented in a real application easily (Moreira *et al.,* 2007), but it is impossible to have a smooth transition between the connected straight lines due to their discontinuous first derivative. This kind of physical constraint, the discontinuity, usually generates overshoots when the ship starts to follow the next segment of the trajectory. In order to reduce the overshoots, some technologies need to be used to smooth the transition area between the connected straight lines. Fossen *et al.,* (2015) presented the integral LOS guidance law for autonomous marine vehicles to follow the Dubins paths, which were usually made of either straight-line or circular arcs, considered as the shortest possible trajectory between the waypoints.

Interpolation techniques can be used to design the paths with continuous curvature. The Lagrange form, which is the most compact representation, will be used to show the interpolating polynomial:

$$P(x)=\sum_{k=1}^{n}\Big(\prod_{j=1,j\neq k}^{n}\frac{x-x_j}{x_k-x_j}\Big)\,y_k \tag{1}$$

where $P(x)$ is defined by the interpolation, as shown in Eq. (1). When x equals x_k, then $P(x_k)=y_k, k=1,\ldots,n$. It means that $P(x)$ will pass exactly through the waypoints. Owing to the fully-degree polynomial interpolation (n-1) defined in (1), it will be hardly or impractically used to produce the path. The geometric shape of the path will change and can even be different when one of the way-points is changed.

The piecewise cubic Hermite polynomial is a robust interpolation method. In Figure.1, the resulting path can connect all points, which also means that when a ship tracks the path, she will travel through all the predefined points. If the coordinate of the last waypoint is changed, it will have no effect on the previous segments of the path, which means that the geometric shape of the path will be stable. By assigning the derivatives of each waypoint, it is possible to get easily the local control along the trajectory. As presented in Moler, (2004), assume h_k as the distance of the adjacent waypoints. and $P(x)$ is a cubic polynomial defined as:

$$P(x)=H(s)\cdot[y_k,y_{k+1},d_k,d_{k+1}]^T \tag{2}$$

where $d_i=P'(x_i)$ is the first derivative of each way-points $(i=k,k+1)$, $s=x-x_k$ are the local variables, which change from x_k to x_{k+1}. The matrix $H(s)$, is the cubic Hermite basis, which is defined by:

$$H(s)=[s^3,s^2,s,1]\cdot\begin{bmatrix}2&-2&h&h\\-3h&2h&-2h^2&0\\0&0&h^3&-h^2\\h^3&0&0&0\end{bmatrix}\cdot\frac{1}{h^3} \tag{3}$$

As discussed above, the 1st order derivatives of the control points or waypoints need to be defined carefully. The right values of derivatives of the control points will avoid or minimise the overshoots along the path, at least locally. The slope, δ_k, is defined by:

$$\delta_k=\frac{y_{k+1}-y_k}{h_k} \tag{4}$$

If the sign of δ_k and δ_{k-1} are opposite or one of them is zero, the 1st order derivative of the control point (x_k,y_k) should be zero ($d_k=0$). If δ_k has the same sign of the δ_{k-1}, then d_k is defined by:

$$\frac{w_1+w_2}{d_k}=\frac{w_1}{\delta_{k-1}}+\frac{w_2}{\delta_k} \tag{5}$$

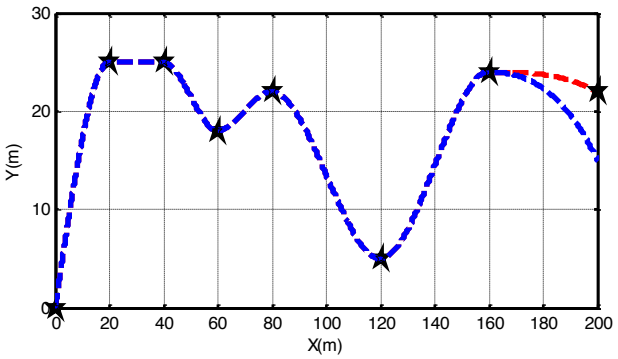

Figure 1: Curved trajectory defined by piecewise cubic Hermite polynomials.

3. GUIDANCE LAWS FOR UNDERACTUATED MARINE SURFACE VEHICLES

In general, commercial ships are equipped with one propeller and rudder, which are responsible for the advance speed control and heading control respectively (Fossen *et al*., 2003; Sutulo and Guedes Soares 2011). This minimum configuration for path following control is one typical underactuated problem (Sutulo and Guedes Soares 2005). In other words, 3 degree of freedom motion behaviour (surge, sway, and yaw) needs to be controlled, but there are only two control inputs available for the control task. The guidance system is thus an important part for underactuated autonomous surface ships. In this section, the LOS and vector field guidance laws for an autonomous ship model are studied. In order to control the ship model to track the predefined trajectory, the guidance laws should have a good ability to reduce the feedback

errors of the system, in the present case, the heading and the cross-track error should be the control parameters.

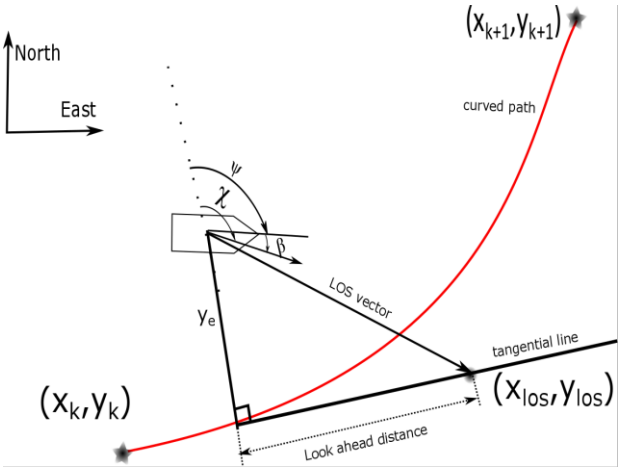

Figure 2: Principle of LOS guidance law for a curved path.

The LOS was widely employed in the application of path-tracking of surface ship models (Breivik and Fossen, 2008). Some modifications will be made here in order to implement LOS in the curved path following case. The principle of LOS is presented in Figure 2, and the main variables are indicated in the figure. The look-ahead distance needs to be defined beforehand, and the LOS guidance law will generate the desired heading angle, which will guide the ship towards the virtual target point (x_{los}, y_{los}). The virtual target point is located on the virtual line with a constant look-ahead distance, which is tangent to the predefined path.

$$\psi_d = \chi^f + \arctan(\frac{-y_e}{\Delta}) - \beta \tag{6}$$

Where, Δ denote the constant distance and β denotes the sideslip angle of the vehicle.

The principle of VF is that it will generate the vectors around the trajectory. The vectors denote the desired course angles for autonomous ship models, as presented in Figure 3-4. As shown in the figure, if the ship travels with the vectors, then it will finally be leading to follow the trajectory. To introduce the principle of VF, without loss of generality, the case of straight path-following will be chosen. It means that χ^f will be kept constant along each segment of the path. The velocity of the ship model can be defined by:

$$\begin{aligned} \dot{x} &= U_r \cos(\chi) \\ \dot{y} &= U_r \sin(\chi) \end{aligned} \tag{7}$$

where, ψ is the heading angle of the autonomous ship model, $\chi = \psi + \beta$ is the course angle and $U_r = \sqrt{u_r^2 + v_r^2}$ is the ship's advance speed.

Algorithms 1: Vector Field guidance law

Initialize: Set $(w_{xj}, w_{yj}), j = 1 \cdots N; \tau \leftarrow 2L_{pp}$; $\chi^e \leftarrow 0.5\pi$;

Result: ψ^d // *desired heading angle*

1. $\chi^f \leftarrow \text{atan}\,2((w_{xj}, w_{yj}), (w_{xj+1}, w_{yj+1}))$; // *calculate heading from waypoint j+1 to j;*
2. $y_e \leftarrow dis\left\|(x,y) - (x_{path}, y_{path})\right\|$; // *the cross-track errors*
3. $\rho \leftarrow sign(y_e)$; // *decide where the ship is;*
4. $d \leftarrow \left\|dis((x,y),(w_{xj+1}, w_{yj+1}))\right\|$ // *the distance from* (w_{xj+1}, w_{yj+1}) ;
5. **If** $d > 2L_{pp}$ **Then**
6. $\quad j \leftarrow j+1$;
7. **End**
8. **If** $|y_e| \geq \tau$ **Then**
9. $\quad \chi^d \leftarrow \chi^f - \rho\chi^e$ // *set vector*
10. $\quad$ *field heading;*
11. $\quad \psi^c \leftarrow \chi^d - \beta$
12. **else**
13. $\quad$
14. $\quad \chi^d \leftarrow \chi^f - \rho\left(\frac{|y_e|}{\tau}\right)^k \chi^e$;
15. $\quad$
16. $\quad \psi^d \leftarrow \chi^d - \left(\frac{k\chi^e U_r}{a\tau}\right)(|y_e|)^{k-1}\sin(\chi) - \beta$
17. **End**
18. **Return** ψ^d

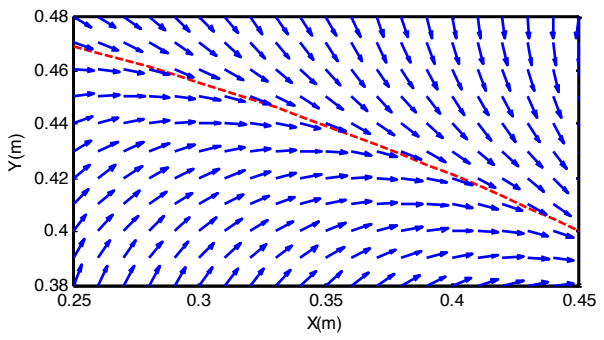

Figure 3: Vectors around the trajectory.

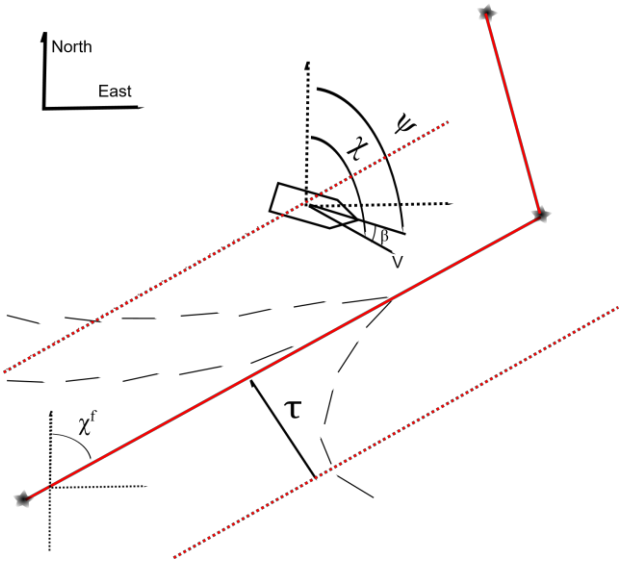

Figure 4: Principle of VF for path-following.

As presented in Figure 4, the red solid line denotes the predefined trajectory. The red dashed line denotes the transition region, which lies on both sides of the predefined path with a distance τ. In order to control the ship, a vector field needs to be constructed around the trajectory. When the ship is located at a distance d, which is greater than τ, the guidance law will control the ship to turn towards the trajectory with a constant entry angle χ^e. This means that the guidance law will control the ship to enter the transition region as quickly as possible. When the ship enters, the commanded heading angle will be determined by the cross-track errors, velocity and heading angle or course angle.

4. NONLINEAR MANOEUVRING MODEL OF AUTONOMOUS VEHICLES

In this section, the modified Abkowitz equation (Abkowitz, 1980) will be presented and used for the simulation study. The current force will be considered as the main environmental disturbance for manoeuvring modelling. The effect of the current can be directly included in the mathematical model. Define u_c as the magnitude of the current, α the direction of the current, u is the forward component of the ground speed, and v is the transverse component. The relative forward velocity u_r and transverse velocity v_r are given by

$$\begin{aligned} u_r &= u - u_c \cos(\psi - \alpha) \\ v_r &= v + u_c \sin(\psi - \alpha) \end{aligned} \tag{8}$$

The time derivatives of u and v are given:

$$\begin{cases} \dfrac{du}{dt} = \dfrac{du_r}{dt} - u_c r \sin(\psi - \alpha) \\ \dfrac{dv}{dt} = \dfrac{dv_r}{dt} - u_c r \cos(\psi - \alpha) \end{cases} \tag{9}$$

where the accelerations of the motion in 3 degree of freedom (surge, sway and yaw) are given by (Xu, *et al.* 2018):

$$\begin{cases} \dfrac{du_r'}{dt} = \dfrac{f_1'}{m' - X_{\dot{u}_r}'} \\ \dfrac{dv_r'}{dt} = \dfrac{1}{f_4'}\left[(I_z' - N_{\dot{r}}')f_2' - (m'x_G - Y_{\dot{r}}')f_3'\right] \\ \dfrac{dr'}{dx} = \dfrac{1}{f_4'}\left[(m' - Y_{\dot{v}_r}')f_3' - (m'x_G - N_{\dot{v}_r}')f_2'\right] \end{cases} \tag{10}$$

where

$$\begin{cases} f_1' = \eta_1' u_r'^2 + \eta_2' n' u_r' + \eta_3' n'^2 - C_R' + X_{v_r}'^2 v_r'^2 + X_{e^2}' e^2 + \left(X_{r^2}' + m' x_G'\right) r'^2 + \left(X_{v_r r}' + m'\right) v_r' r' + X_{v_r^2 r^2}' v_r'^2 r'^2 \\ f_2' = Y_0' + \left\{Y_{v_r}' v_r' + Y_\delta' (c - c_0) v_r'\right\} + \left\{\left(Y_r' - m' u_r'\right) r - -\dfrac{Y_\delta'}{2}(c - c_0) r'\right\} + Y_\delta' \delta + Y_{r^2 v_r}' r'^2 v_r' + Y_{e^3}' e^3 \\ f_3' = N_0' + \left\{N_{v_r}' v_r' - N_\delta' (c - c_0) v_r'\right\} + \left\{\left(N_r' - m' x_G' u_r'\right) r + \dfrac{1}{2} N_\delta' (c - c_0) r'\right\} + N_\delta' \delta + N_{r^2 v_r}' r'^2 v_r' + N_{e^3}' e^3 \\ f_4' = \left(m' - Y_{\dot{v}_r}'\right)\left(I_z' - N_{\dot{r}}'\right) - \left(m' x_G' - N_{\dot{v}_r}'\right)\left(m' x_G' - Y_{\dot{r}}'\right) \end{cases} \tag{11}$$

In Eqs. (11), in order to describe the surge motion, f_1 can be divided into two components. It means that:

$$\text{Thrust}\,(u_r,n)=\left[\frac{\rho}{2}L^2\right]\eta_1' u_r^2+\left[\frac{\rho}{2}L^3\right]\eta_2' n u_r+\left[\frac{\rho}{2}L^4\right]\eta_3' n^2 \tag{12}$$

$$f_1(u_r,v_r,u,v,r,\delta)=-C_R'\left[\frac{\rho}{2}Su_r^2\right]+X_{v_r^2}'\left[\frac{\rho}{2}L^2\right]v_r^2+X_{e^2}'\left[\frac{\rho}{2}L^2c^2\right]e^2+\left(X_{r^2}'+m'x_G'\right)\left[\frac{\rho}{2}L^4\right]r^2+\left(X_{v_r r}'+m'\right)\left[\frac{\rho}{2}L^3\right]v_r r+X_{v_r^2 r^2}'\left[\frac{\rho}{2}L^4U^{-2}\right]v_r^2 r^2 \tag{13}$$

where ρ is the density of seawater, n is the propeller's rotating speed (rpm), S is the wetted surface area, C_R is the resistance coefficient and e is the effective rudder angle defined by:

$$e=\delta\frac{v}{c}+\frac{rL}{2c} \tag{14}$$

and c is the weighted average flow velocity over rudder given by

$$c=\sqrt{\frac{A_P}{A_R}[(1-\omega)u_r+ku_{A\infty}]^2+\frac{A_R-A_P}{A_R}(1-\omega)^2u_r^2} \tag{15}$$

where $u_{A\infty}$ is the induced axial velocity behind the propeller disk, which is defined by

$$u_{A\infty}=(1-w)u+\sqrt{(1-w)^2u^2+\frac{8}{\pi}K_T(nD)^2} \tag{16}$$

The non-dimensional hydrodynamic coefficients of "Esso Osaka" adapted from Moreira *et al*., (2007) will be used in the simulation. The length of the ship model is 3.4m, the breadth is 0.5m and the draught is 0.22m. It is installed with one propeller and one rudder. The speed is 0.41m/s. This model is quite comprehensive and has been validated with the sea trials. It gives highly realistic results. The coefficients are presented in Table 1. In order to carry out the parameter identification of the 2nd order Nomoto model, the manoeuvring test needs to be carried out. The $20^\circ-20^\circ$ zigzag manoeuvre has been carried out based on the previous discussed mathematical model. The rudder angle and heading angle during the manoeuvring test are recorded and presented in Figure. 5

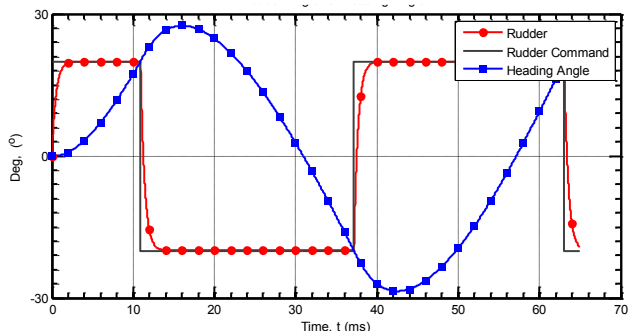

Figure 5: $20^\circ-20^\circ$ zigzag manoeuvring test for "*Esso Osaka*" model.

Table 1. Non-dimensional hydrodynamic coefficients of "*Esso Osaka*"

Coefficient	Value	Coefficient	Value
$(m-Y_{\dot v})'$	0.0352	Y_0'	1.90*e-6
$(I_z-N_{\dot r})'$	0.00222	Y_{v_r}'	-0.0261
$(m-X_{\dot u_r})'$	0.0116	Y_δ'	0.00508
η_1'	-0.962*e-5	Y_r'	0.00365
η_2'	-0.446*e-5	Y_{rrv_r}'	-0.0450
η_3'	0.0309*e-5	Y_{eee}'	-0.00185
C_R'	0.00226	N_0'	-0.00028
$X_{v_r^2}'$	-0.006	N_{v_r}'	-0.0105
X_{ee}'	-0.00224	N_δ'	-0.00283
X_{rr}'	0.00515	N_r'	-0.00480
$(X_{v_r r}+m)'$	0.0266	N_{rrv_r}'	0.00611
X_{rrvv}'	-0.00715	N_{eee}'	0.00116

5. VYSHNEGRADSKY DIAGRAM FOR AUTOPILOT DESIGN AND PARAMETERS ESTIMATION

5.1 AUTOPILOT DESIGN USING VYSHNEGRADSKY DIAGRAM

In order to design the autopilot for ASVs, the 1st order Nomoto model was widely used in practical applications (Fossen, 2011). It is a simple form for control purposes, sometimes over-simplified leading to failure to give satisfying results and also cannot reproduce the time response of yawing angle. In this part, the 2nd order Nomoto model will be introduced for heading controller design. The 2nd order Nomoto model is described by:

$$\begin{aligned}\dot\psi&=r\\ T_1T_2\ddot r+(T_1+T_2)\dot r+r&=K\delta+KT_3\dot\delta\end{aligned} \tag{16}$$

where T_i and K are the time lag and gain, respectively $(i=1,2,3)$. Considering a PD control law in the form (Fossen, 2011):

$$\delta=K_p(\psi_d-\psi)-K_d\dot\psi \tag{17}$$

where ψ_d and ψ are the desired heading angle and real-time heading angle, respectively and $K_p > 0$ and $K_d > 0$ are the parameters of controller. Closing the loop considering the ship dynamics and controller,

$$T_1T_2\dddot{\psi} + \left(T_1 + T_2 + KT_3K_d\right)\ddot{\psi} + \left(1 + KK_d + KT_3K_p\right)\dot{\psi} + KK_p\psi = KK_p\psi_d \tag{18}$$

Rewriting the equation in the frequency domain, leads to:

$$\frac{T_1T_2}{KK_p}s^3 + \frac{\left(T_1 + T_2 + KT_3K_d\right)}{KK_p}s^2 + \frac{\left(1 + KK_d + KT_3K_p\right)}{KK_p}s + 1 = 0 \tag{19}$$

Assume $s = \sqrt[3]{KK_p / T_1T_2}\ q$, then

$$q^3 + As^2 + Bs + 1 = 0 \tag{20}$$

where A>0, B>0 and AB>1

$$\begin{cases} A = \dfrac{1}{\left(T_1T_2\right)^{2/3}} \dfrac{\left(T_1 + T_2 + KT_3K_d\right)}{\left(KK_p\right)^{1/3}} \\ B = \dfrac{1}{\left(T_1T_2\right)^{1/3}} \dfrac{\left(1 + KK_d + KT_3K_p\right)}{\left(KK_p\right)^{2/3}} \end{cases} \tag{21}$$

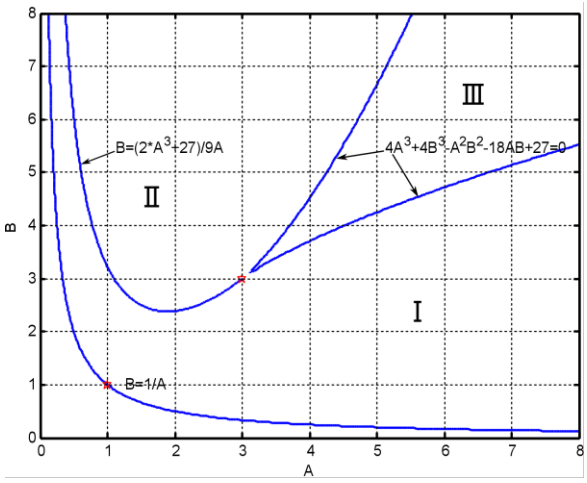

Figure 6: Diagram of Vyshnegradsky.

The diagram of Vyshnegradsky (DV) (Figure 6), received subsequently its name, recognizing Ivan Vyshnegradsky, who for the first time constructed it in 1876 in the work that originated the automatic regulation theory (Alekseevich and Mironovskii, 2011). The factors (A, B) are the Vyshnegradsky parameters. As shown in Figure 5, the stability of the control system will be determined by the parameters. For example, if the parameters (A, B) are located under the line $(A*B=1)$, the control process will be unstable and cannot converge. Usually, the coordinate $(3,3)$ will be the ideal value. However, considering the parameters drift due to environmental disturbances, the parameters $(A=4, B=4)$ will be used for the autopilot design of the autonomous ship model in this paper.

5.2 PARAMETER IDENTIFICATION BASED ON SUPPORT VECTOR MACHINE

In the following section, a parameter estimation method will be employed to obtain the parameters. Different parameter estimation methods have been used in modelling ships' motion. Sutulo and Guedes Soares (2015), used an offline algorithm to identify the ship manoeuvring model based on free-running tests. A classical genetic algorithm (GA) was employed for minimizing the cost functions, which were established based on different metrics, such as Euclidean metric, Abs-metric, and Hausdorff metric. Perera *et al.* (2016) applied an extended Kalman filter to identify a nonlinear ocean vessel steering model. Recently Support Vector Machine (Falck *et al.*, 2012; Luo, *et al*, 2016; Xu et al. 2019c, 2020a, 2020b, 2020c) have been used to obtain the parameters of a manoeuvring model.

The parameters of the 2nd order Nomoto model will be obtained based on Least Square Support Vector Machine in this work. For regression purposes, support vector machine can be expressed in a general approximation function form:

$$y = w^T \cdot \Phi(x) + b \tag{22}$$

in which, x is the training sample or input, $x \subset R^n$, y is the target value or output, $y \subset R$ $w^T \cdot \Phi(x) + b$ is the prediction for that sample, w is a weight matrix, b is the bias term and $\Phi(\cdot)$ is a nonlinear kernel function, which can map the training sample to a high dimension space. The performance of the estimation method can be evaluated by hypothesis space complexity and the empirical error is also known as structural risk. It provides a trade-off between structure complexity and empirical errors. A cost function can be defined as follows:

$$\begin{cases} \min_{w,b,e} f(w,e) = \dfrac{1}{2}w^Tw + \dfrac{1}{2}C\sum_{i=1}^{l} e_i^2 \\ subject\ to: y_i = w^T \cdot \Phi(x_i) + b + e_i \end{cases} \tag{23}$$

where C is the regularization factor and e_i, $i = 1 \cdots l$ are error variables. The minimization of w^Tw is closely related to the use of a weight decay term in the training of neural networks, and the $\sum_{i=1}^{l} e_i^2$ controls the empirical errors. The Lagrangian function can be constructed as:

$$\mathcal{L}(w,b,e,\alpha)=\frac{1}{2}w^{T}w+\frac{1}{2}C\sum_{i=1}^{l}e_i^{2} -\sum_{i=1}^{l}\alpha_i[w^{T}\cdot\Phi(x_i)+b+e_i-y_i] \quad (24)$$

where α_i are the Lagrange multipliers. Deriving Eq. (24) with respect to ω,b,e,α , leads to:

$$\begin{cases} \dfrac{\partial\mathcal{L}}{\partial w}=0 \;\rightarrow\; w=\sum_{i=1}^{l}\alpha_i\Phi(x_i) \\ \dfrac{\partial\mathcal{L}}{\partial b}=0 \;\rightarrow\; \sum_{i=1}^{l}\alpha_i=0 \\ \dfrac{\partial\mathcal{L}}{\partial e_i}=0 \;\rightarrow\; \alpha_i=Ce_i \\ \dfrac{\partial\mathcal{L}}{\partial \alpha_i}=0 \;\rightarrow\; w^{T}\cdot\Phi(x_i)+b+e_i-y_i=0 \end{cases} \quad (25)$$

It is necessary to eliminate the variables ω and e_i in Eq. (25), then to apply the kernel function. The kernel functions can work in high-dimensional spaces, without introducing explicit computations. For function estimation purpose, the Least Square Support Vector Method can be defined by

$$y(x)=\sum_{i=1}^{l}\alpha_i K(x,x_i)+b \quad (26)$$

where $K(x,x_i)$ is an inner product between its operands, also known as the kernel function. The kernel function is positive definite with the Mercer condition. In this paper, a linear kernel function will be used to estimate the parameters of the 2nd order Nomoto model, given:

$$T_1T_2\ddot{r}+(T_1+T_2)\dot{r}+r=K\delta+KT_3\dot{\delta} \quad (27)$$

So $x=[r_k,\dot{r}_k,\delta_k,\dot{\delta}_k]$ is the training sample, and $y=[\dot{r}_{k+1}]$ is the target value. From the previous discussion, the regularization factor needs to be chosen carefully. Following Luo et al., (2016), the regularization factor C= *2544* was chosen.

The Nomoto parameters (T_1,T_2,T_3,K) will need to be identified. The $20^{\circ}-20^{\circ}$ zigzag simulation results will feed into the identification system. The results are: K=0.185s^{-1}, T_1=7.8569 s, T_2=0.3815 s, T_3=0.5297 s. As shown in Figure 7, the identification results agree very well with the data. According to the equation (21), the control parameters can be derived, and the values are 212.6 and 547.8, respectively. To reduce the accumulated errors, the PD controller will be modified, and an integral part should be included. The value K_i will be set to $K_p/100$.

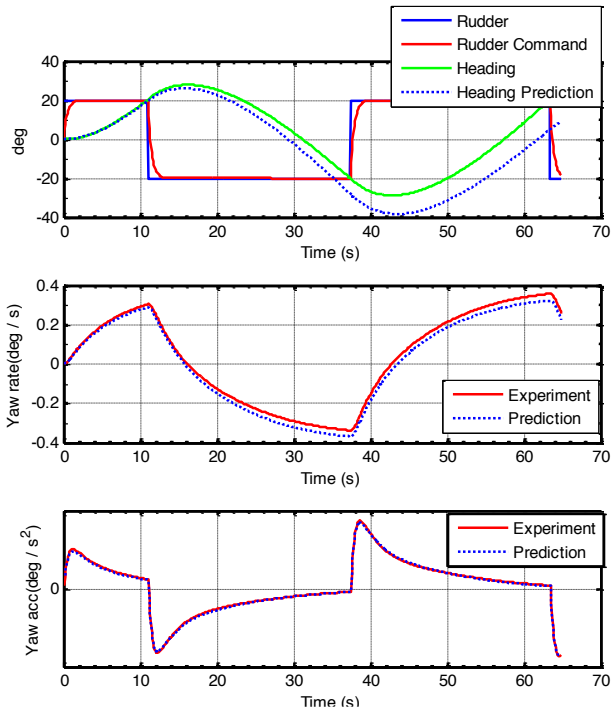

Figure 7: Prediction of $20^{\circ}-20^{\circ}$ Zigzag manoeuvre.

6. SIMULATION STUDY

The performance and effectiveness of the VF path-following guidance law will be validated in the section. The non-linear manoeuvring model and model-based PID controller will be used in the program. The "Esso Osaka" model will be the ASV's prototype considering the rich experimental data already available about it. Some previous works on autonomous ship model have been done based on a scaled "Esso Osaka" model (Moreira *et al.*, 2007). The Labview platform has been used for developing the guidance, navigation and control system (GNC). The autonomous ship model will be capable of carrying various manoeuvring tests (Moreira and Guedes Soares, 2014).

6.1 STRAIGHT PATH FOLLOWING USING LOS AND VF

Firstly, straight-line following simulation tests will be demonstrated for comparing the performance of the proposed guidance laws. In this case the path is constructed with 4 waypoints, which are connected with straight lines. The initial position of the autonomous surface vehicle is the original point and the heading is zero. The information of the trajectory is presented in Figure 8 and the desired speed will be kept constant, V= 0.41m/s (*Fn=0.0744*).

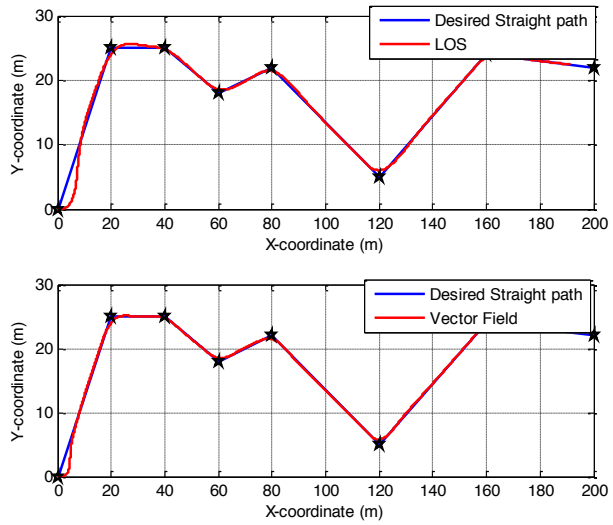

Figure 8: Straight path following of autonomous ship model using LOS and VF.

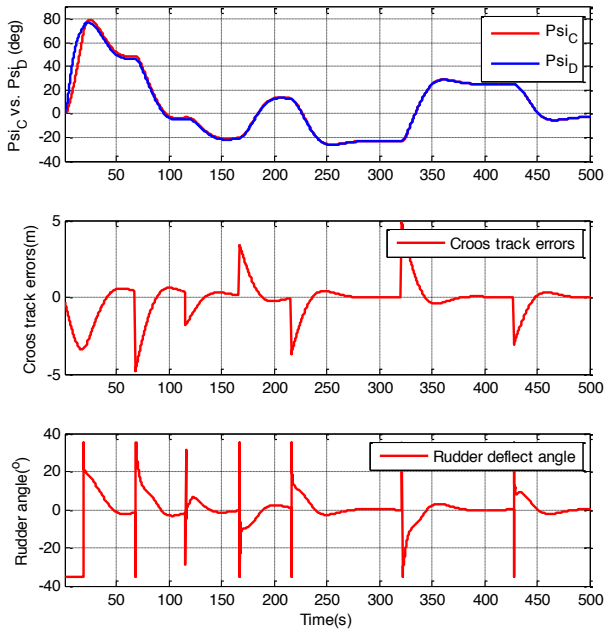

Figure 9: Heading angles, cross-track errors and rudder deflect angles in the process of the ASV flowing the predefined straight line path using LOS.

The simulation results can be found in Figures 8-10. Figure 8 shows the geometry of the predefined trajectory and the real-time location of the autonomous surface vehicle. The two guidance laws, LOS and VF, can control the vehicles to track the predefined trajectory successfully, which can also be demonstrated in Figure 8. It can be concluded from the graph that LOS guidance law results in some overshoots due to the large velocity, especially in the transition area. This phenomenon can be avoided when the speed is small. The cause is rooted in the definition of the LOS guidance law, in which the motion of the vehicles is not considered. The desired heading of the ship model is generated based on the VF guidance law, which includes the velocity and drift angle of the vehicles during the process. So it can avoid the large overshoots when the ship is tracking the next way-point, as shown in Figure 8. This feature is also demonstrated in Table 2. The autonomous surface vehicles using VF have a smaller mean value of cross-track errors.

The heading angles, cross-track errors and rudder deflection angles of the autonomous surface vehicles based on LOS guidance law are demonstrated in Figure 9. The real-time heading angle can track the desired heading angle successfully, which will allow the vehicles to track the predefined trajectory. The absolute value of the cross-track error is less than 5 m, which can be acceptable in practical applications.

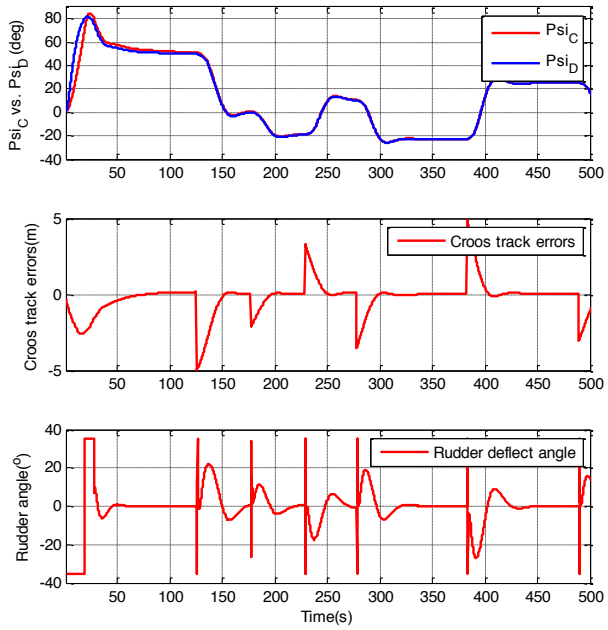

Figure 10: Heading angles, cross-track errors and rudder deflection in the process of the ASV flowing the predefined straight-line path using VF.

In Figure10, the heading angles, cross-track errors and rudder deflection angles of the autonomous surface vehicles based on vector field guidance law are shown. As shown in Figures 8 and 10, the vector field algorithm can control the ASVs following the predefined trajectory successfully. In Figure 10, the real-time heading angle agrees well with the desired heading angle. The cross-track errors are limited to a reasonable range (±5m). Table 2 gives the complete list of the statistical parameters (mean value and standard deviation) of LOS and VF. The mean values and standard deviation of both guidance laws are similar, it means that both guidance laws have similar performance for straight-line path following. It can be concluded that the LOS and VF guidance laws can guide the autonomous ship model successfully with acceptable errors.

Table 2. Statistical features of LOS and VF for straight path following

	Mean Value		Standard Deviation	
	LOS	VF	LOS	VF
Cross-track errors	0.64	0.53	0.96	0.95
Heading errors	1.13	1.25	3.26	3.67
Rudder	4.61	5.32	7.78	8.90

6.2 CURVED PATH FOLLOWING BASED ON LOS AND VECTOR FIELD GUIDANCE LAWS

The curved path following simulations is carried out in this section for validating the previously discussed guidance laws, LOS and Vector Field. The trajectory is made of smooth curved lines, which are generated using piecewise cubic Hermite polynomials. As previously mentioned, the derivative at each waypoint affects the overall shape of the trajectory. In the present study, the 1st derivative will take values considering the coordinates of the nearby way-points.

The same trajectory will be used for the curved path-following case. The coordinates of each way-point will be the same. The initial velocity of the autonomous surface vehicle is V= 0.1m/s (Fn=0.0186). The simulation results can be found in Figures 11-13. The geometry of curved-path and real-time locations of the autonomous surface ship model is shown in Figure 11. The curved path connects all way-points without the large overshoot and wiggles. As shown in Figure 11, the two guidance laws, LOS and VF, can guide the vehicles to track the curved trajectory successfully.

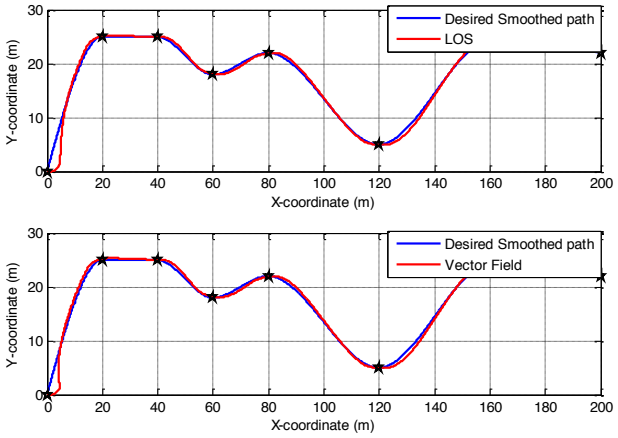

Figure 11: The geometry of curved path-following using LOS and VF.

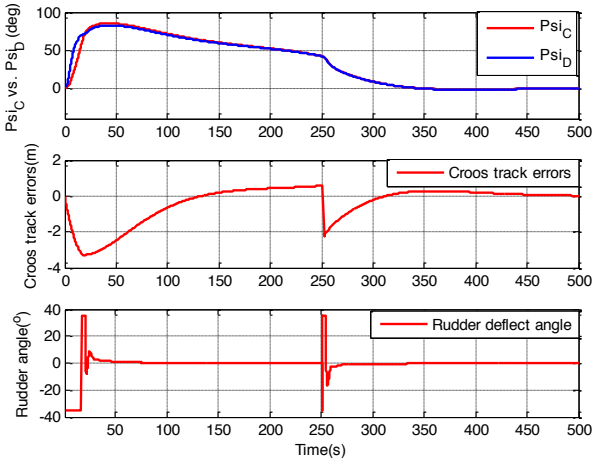

Figure 12: The heading angles, cross-track errors and rudder deflect angles in the process of the ASV flowing the curved path using LOS.

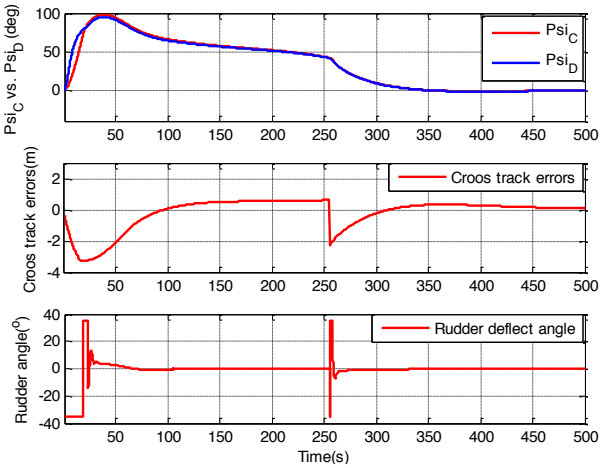

Figure 13: The heading angles, cross-track errors and rudder deflect angles in the process of the ASV flowing the curved path using VF.

The heading angles, cross-track errors and rudder deflection angles of the autonomous surface vehicles based on LOS guidance law are shown in Figure 12. In this figure, the real-time heading angle agrees well with the desired heading angle. The ship follows the trajectory with small cross-track errors, which falls within the margin of error, in the range of -3m and 2m. Comparing with the Figure 9, the cross-track error is reduced when the vehicle follows the curved path. The significant improvement is the rudder deflection angle. In Figure 12, there are only two steep oscillations of rudder angle, which occurred at the beginning and large turn moments. That means, for autonomous surface vehicles control systems, following a curved path will give more stable inputs. This is what is desired for autonomous vehicles because large oscillation of inputs will lead to unnecessary control output, which usually will make the ship unstable and take more energy.

The heading angles, cross-track errors and rudder deflection of autonomous surface vehicles based on vector field guidance law are demonstrated in Figure 13. In this figure, the desired heading angle generated using the VF guidance law is smoother, and the real-time heading angle agrees well. The cross-track errors are small and more stable and limited in a reasonable range (change from -3m to 1m). The rudder deflection angles are also very stable. So, the Vector Field guidance law is a good means for path following control of autonomous surface ship models. Table 3 gives the complete lists of the statistical parameters (mean value and standard deviation) of LOS and VF guidance law. From this table, the mean values of the cross-track error and rudder angle are the same, but the standard deviation is smaller for VF guidance law. It indicates that the VF is more stable. So, the VF guidance law is recommended when the path is cured. From Table 2 and Table 3, one can conclude that the autonomous surface vehicle can cross all predefined points and follow a smooth path with small errors. It is important for autonomous surface vehicles owing to its limited energy reserves on board.

Table 3. Statistical features of LOS and VF guidance law for curved path following

	Mean Value		Standard Deviation	
	LOS	VF	LOS	VF
Cross-track errors	0.40	0.42	0.51	0.47
Heading errors	0.32	0.37	1.96	2.12
Rudder	0.88	0.88	4.14	0.91

7. CONCLUSION

In this paper, piecewise cubic Hermite polynomials have been presented and used for curved path generation. The resulting trajectory can pass through all control points or waypoints with 1st order derivative continuity. This trajectory is stable, at least locally, and without unnecessary over-shoots and wiggles. The VF and look-ahead LOS guidance laws have been implemented in the guidance system of the autonomous ship model. The principle of VF is that it produces the vectors around the trajectory, which indicate the desired course angles for the controller. The 2nd order Nomoto model has been used to design the autopilot for the autonomous ship model. Least square support vector method was used for the parameters identification (time lags and gain). The PID parameters have been derived based on Vyshnegradsky Diagram technology. The performance of VF and look-ahead LOS guidance laws have been demonstrated in the simulation tests in which a nonlinear manoeuvring model was implemented.

The results show that the VF and look-ahead LOS are effective and can control the underactuated marine ship model to pass through the predefined waypoints. Both guidance laws can achieve similar performance for straight-line path-following. For curved path following, the VF guidance law is more stable. The cross-track errors and heading errors change in a reasonable range. It confirmed that the autonomous surface vehicle can follow the curved path successfully based on the proposed algorithms with smaller cross-track errors, heading errors, and consume less energy than other methods, which demonstrate the benefits of the vector field guidance law

8. ACKNOWLEDGEMENTS

This work was performed within the Strategic Research Plan of the Centre for Marine Technology and Ocean Engineering (CENTEC), which is financed by Portuguese Foundation for Science and Technology (Fundação para a Ciência e Tecnologia - FCT) under contract UIDB/UIDP/00134/2020.

9. REFERENCES

1. ABKOWITZ, M. A. *Measurement of hydrodynamic characteristics from ship maneuvring trials by system identification*. SNAME Transactions, 88, 283–318. (1980)
2. ALEKSEEVICH, L., MIRONOVSKII, T.N.S., *On the properties of regular dynamical systems*. Problemy Upravleniya 3, 12–19. (2011).
3. BROWN, M., FUNKE, J., ERLIEN, S., GERDES, J.C., *Safe driving envelopes for path tracking in autonomous vehicles*. Control Engineering Practice, 61, 307-316. (2016)
4. BRUYNINCKX, H., REYNAERTS, D., *Path planning for mobile and hyper-redundant robots using Pythagorean hodograph curves*, in: 8th International Conference on Advanced Robotics. Proceedings. ICAR'97. IEEE, 595–600. (1997)
5. CHEN, C., SHIOTANI, S., SASA, K., *Numerical ship navigation based on weather and ocean simulation.* Ocean Engineering. 69, 44–53. (2013)
6. DUBINS, L.E., *On Curves of Minimal Length with a Constraint on Average Curvature, and with Prescribed Initial and Terminal Positions and Tangents*. American Journal of mathematics, 79(3), 497–516. (1957)
7. FALCK, T., DREESEN, P., DE BRABANTER, K., PELCKMANS, K., DE MOOR, B., SUYKENS, J.A.K., *Least-Squares Support Vector Machines for the identification of Wiener–Hammerstein systems*. Control Engineering Practice, 20, 1165–1174. (2012)
8. FAROUKI, R.T., SAKKALIS, T., *Pythagorean hodographs*. IBM Journal of Research and Development. 34, 736–752. (1990)
9. FOSSEN, T., BREIVIK, M., SKJETNE, R., *Line-of-sight path following of underactuated marine craft*, in: Proceedings of the 6th IFAC MCMC, Girona, Spain. 244–249. (2003)

10. FOSSEN, T.I., *Handbook of Marine Craft Hydrodynamics and Motion Control, Handbook of Marine Craft Hydrodynamics and Motion Control*. John Wiley & Sons Ltd. (2011)
11. FOSSEN, T.I., PETTERSEN, K.Y., GALEAZZI, R., *Line-of-sight path following for dubins paths with adaptive sideslip compensation of drift forces*. IEEE Transactions on Control Systems Technology, 23, 820–827. (2015)
12. GONÇALVES, V.M., PIMENTA, L.C.A., MAIA, C.A., DUTRA, B.C.O., PEREIRA, G.A.S., *Vector fields for robot navigation along time-varying curves in n-dimensions*. IEEE Transactions on Robotics, 26(4), 647–659. (2010)
13. HINOSTROZA, M. A., XU, H., & GUEDES SOARES, C. *Cooperative operation of autonomous surface vehicles for maintaining formation in complex marine environment*. *Ocean Engineering*, *183*, 132–154. (2019)
14. JIAN, C., JIAYUAN, Z., FENG, X., JIANCHUAN, Y., ZAOJIAN, Z., HAO, Y., TAO, X., LUCHUN, Y., *Parametric estimation of ship maneuvering motion with integral sample structure for identification.* Applied Ocean Research, 52, 212–221. (2015)
15. LEKKAS, A. M; DAHL, A.R.; BREIVIK, M.; FOSSEN, T.I., *Continuous-curvature path generation using Fermat's spiral*. Modeling, Identification and Control, 34(4),183–198. (2013)
16. LEKKAS, A.M., FOSSEN, T.I., *Integral LOS Path Following for Curved Paths Based on a Monotone Cubic Hermite Spline Parametrization*. IEEE Transactions on Control Systems Technology, 22, pp. 2287–2301. (2014)
17. LEKKAS, A.M., FOSSEN, T., *Line-of-sight guidance for path following of marine vehicles*. Advanced in marine robotics, 63–92. (2013)
18. LIM, S., JUNG, W., BANG, H., *Vector field guidance for path following and arrival angle contro*l, in: 2014 International Conference on Unmanned Aircraft Systems, ICUAS 2014 - Conference Proceedings. 329–338. (2014)
19. LJUNG, L., *System Identification: Theory for User*, Prentice-Hall. Englewood Cliffs, N.J. (1987)
20. LOE, Ø., *Collision Avoidance for Unmanned Surface Vehicles*. Norwegian University of Science and Technology. (2008)
21. LUO, W.L., GUEDES SOARES, C., and ZOU, Z., *Parameter Identification of Ship Maneuvering Model Based on Support Vector Machines and Particle Swarm Optimization*. Journal of Offshore Mechanics and Arctic Engineering, 138, 131101. (2016)
22. MCGOOKIN, E.W., MURRAY-SMITH, D.J., LI, Y., FOSSEN, T.I., *Ship steering control system optimisation using genetic algorithms*. Control Engineering Practice, 8, 429–443. (2000)
23. MICHAŁEK, M.M., *A highly scalable path-following controller for N-trailers with off-axle hitching*. Control Engineering Practice, 29, 61–73. (2014)
24. MOLER, C., *Numerical Computing with MATLAB*. SIAM, Philadelphia. (2004)
25. MORAWSKI, L., POMIRSKI, J., *Ship track-keeping: experiments with a physical tanker model*. Control Engineering Practice, 6, 763–769. (1998)
26. MOREIRA, L., GUEDES SOARES, C., *Autonomous Ship Model to Perform Manoeuvring Tests*. Journal of Maritime Research, 8(2), 29–46. (2014)
27. MOREIRA, L., FOSSEN, T.I., GUEDES SOARES, C., *Path following control system for a tanker ship model*. Ocean Engineering, 34, 2074–2085. (2007)
28. MORENO-SALINAS, D., CHAOS, D., DE LA CRUZ, J.M., ARANDA, J., *Identification of a surface marine vessel using LS-SVM*. Journal of Applied Mathematics, 1-13. (2013)
29. NELSON, D.R., BARBER, D.B., MCLAIN, T.W., BEARD, R.W., *Vector field path following for small unmanned air vehicles*. In American Control Conference, 2006, 5788–5794. (2006)
30. NELSON, D.R., BARBER, D.B., MCLAIN, T.W., BEARD, R.W., *Vector field path following for miniature air vehicles*. IEEE Transactions on Robotics, 23(3), pp. 519–529. (2007)
31. PERERA, L. P. and GUEDES SOARES, C. *Pre-filtered Sliding Mode Control for Nonlinear Ship Steering Associated with Disturbances.* Ocean Engineering. 51:49-62. (2012).
32. PERERA, L. P.; OLIVEIRA, P., and GUEDES SOARES, C. *System Identification of Vessel Steering with Unstructured Uncertainties by Persistent Excitation Maneuvers*. IEEE Journal of Oceanic Engineering, 41(3), 515-528. (2016)
33. PRPIĆ-ORŠIĆ, J., VETTOR, R., FALTINSEN, O.M., GUEDES SOARES, C., *The influence of route choice and operating conditions on fuel consumption and CO2 emission of ships*. Journal of Marine Science and Technology, 21(3), 1–24. (2016)
34. RONG, H., TEIXEIRA, A. P., & GUEDES SOARES, C. *Ship trajectory uncertainty prediction based on a Gaussian Process model*. *Ocean Engineering*, *182*, 499–511. (2019)
35. SATO, Y., ISHII, H., *Study of a collision-avoidance system for ships*. Control Engineering Practice, 6(9), 1141–1149. (1998)
36. SHIN, J., HUH, J., PARK, Y., *Asymptotically stable path following for lateral motion of an unmanned ground vehicle*. Control Engineering Practice, 40, 102–112. (2015)
37. SUJIT, P.B., SARIPALLI, S., SOUSA, J.B., *Unmanned Aerial Vehicle Path Following: A*

Survey and Analysis of Algorithms for Fixed-Wing Unmanned Aerial Vehicles. IEEE Control Systems, 34(1), 42–59. (2014)

38. SUTULO, S. and GUEDES SOARES, C. *Numerical Study of Some Properties of Generic Mathematical Models of Directionally Unstable Ships*. Ocean Engineering. 32(3),485-497. (2005)
39. SUTULO, S. and GUEDES SOARES, C. *Mathematical models for simulation of manoeuvring performance of ships*. Guedes Soares, C. Garbatov Y. Fonseca N. & Teixeira A. P., (Eds.). Marine Technology and Engineering. London, UK: Taylor & Francis Group; pp. 661-698. (2011)
40. SUTULO, S., GUEDES SOARES, C., *Offline system identification of ship manoeuvring mathematical models with a global optimization algorithm*, in: MARSIM 2015. Newcastle University, United Kingdom, pp. 8–11. (2015)
41. TECHY, L., WOOLSEY, C. A., *Minimum-Time Path Planning for Unmanned Aerial Vehicles in Steady Uniform Winds*. Journal of guidance, control, and dynamics, 32(6), 1736–1746. (2009)
42. VETTOR, R. and GUEDES SOARES, C. *Development of a ship weather routing system.* Ocean Engineering. 2016; 123:1-14.
43. VELAGIC, J., VUKIC, Z., OMERDIC, E., *Adaptive fuzzy ship autopilot for track-keeping*. Control Engineering Practice, 11(4), 433–443. (2003)
44. WU, S.-F., MEI, J.-S., NIU, P.-Y., *Path guidance and control of a guided wheeled mobile robot*. Control Engineering Practice, 9, 97–105. (2001)
45. XU, H.T., GUEDES SOARES, C., *An optimized energy-efficient path following algorithm for underactuated marine surface ship model*. International Journal of Maritime Engineering, 160, 411–421. (2018)
46. XU, H.T., GUEDES SOARES, C., *Vector field path following for surface marine vessel and parameter identification based on LS-SVM*. Ocean Engineering, 113, pp. 151–161. (2016)
47. XU, H. T., HINOSTROZA, M. A. AND GUEDES SOARES, C. *Estimation of Hydrodynamic Coefficients of a Nonlinear Manoeuvring Mathematical Model with Free-Running Ship Model Tests*, International Journal of Maritime Engineering, 160, 213–226. (2018)
48. XU, H., FOSSEN, T.I., GUEDES SOARES, C., *Uniformly semiglobally exponential stability of vector field guidance law and autopilot for path-following.* Eur. J. Control 53, 88–97.(2019a)
49. XU, H., RONG, H., GUEDES SOARES, C., *Use of AIS data for guidance and control of path-following autonomous vessels*. Ocean Eng. 194, 106635. (2019b)
50. XU, H., HASSANI, V., GUEDES SOARES, C., *Uncertainty analysis of the hydrodynamic coefficients estimation of a nonlinear manoeuvring model based on planar motion mechanism tests*. Ocean Eng. 173, 450–459. (2019c)
51. XU, H., GUEDES SOARES, C., *Manoeuvring modelling of a containership in shallow water based on optimal truncated nonlinear kernel-based least square support vector machine and quantum-inspired evolutionary algorithm*. Ocean Eng. 195, 106676. (2020a)
52. XU, H., HINOSTROZA, M. A., WANG, Z., & GUEDES SOARES, C. *Experimental investigation of shallow water effect on vessel steering model using system identification method*. Ocean Engineering, 199, 106940. (2020b)
53. XU, H., HASSANI, V., & GUEDES SOARES, C. *Truncated least square support vector machine for parameter estimation of a nonlinear manoeuvring model based on PMM tests. Applied Ocean Research*, *97*, 102076. (2020c).
54. ZHANG, X.G., ZOU, Z.J., *Identification of Abkowitz model for ship manoeuvring motion using ε-support vector regression*. Journal of hydrodynamics, 23(3), 353–360. (2011)
55. ZHENG, Z., HUO, W., WU, Z., *Autonomous airship path following control: Theory and experiments*. Control Engineering Practice, 21, 769–788. (2013)